IEEE Access
Multidisciplinary | Rapid Review | Open Access Journal

Received July 3, 2019, accepted July 26, 2019, date of publication July 30, 2019, date of current version August 13, 2019.

Digital Object Identifier 10.1109/ACCESS.2019.2932013

The Hybrid Model for Lane-Changing Detection at Freeway Off-Ramps Using Naturalistic Driving Trajectories

TING XU, CHANGLEI WEN, LEI ZHAO, MEIJUN LIU, AND XIANG ZHANG
School of Automobile, Chang'an University, Xi'an 710064, China

Corresponding author: Changlei Wen (2018122097@chd.edu.cn)

This work was supported in part by the National key Research and Development plan of China under Grant 2017YFC0803900, in part by the National Nature Science Foundation of China under Grant 51878066, and in part by the Funds for Central Universities and Colleges of Chang'an University under Grant 300102229201.

ABSTRACT In order to promote traffic safety at freeway off-ramps, this paper designed a hybrid model to identify a lane-changing with vision technology. The unmanned aerial vehicle was used to collect video stream data at five off-ramps for Xi'an Raocheng freeway during weekdays. The positional information-of-an individual vehicle is recorded at a frequency of 5 Hz. Each trajectory is composed of 30 positional records and all trajectories are divided into lane-changing and lane-keeping units. Features such as lateral driving speed, lane departure, and the lane deviation angle extracted from trajectory records are related to the lane-changing behaviors. We develop a hybrid model of the Gaussian Mixture Model and the Continuous Hidden Markov Model to identify lane-changing behaviors at off-ramps with these features. Basing on test set, we conduct a test for the hybrid model and the result shows that the prediction accuracy of the proposed model is as high as 94.4% for lane-changing behavior and 93.6% for lane-keeping behavior.

INDEX TERMS Continuous Hidden Markov Model, freeway off-ramps, hybrid model, lane-changing, naturalistic driving trajectories.

I. INTRODUCTION

Numerous traffic accidents caused by improper driving behaviors, resulting in casualties and extensive property losses. More than 70% of road traffic accidents are caused by unsafe driving behaviors according to the annual road accidents report in China 2016 [1]. 4% to 7% of road traffic accidents in China are caused by improper lane-changing behavior [2]. However, this situation is more exiguous in the US, with 27% of accidents being the result of faulty lane-changing [3]. Freeway off-ramps are the sites of more crashes than other segments, due to the interference of lane-changing [4], [5].

Therefore, many researchers focus on the research of lane-changing behavior for various types of road. The arrangement of off-ramps affects driving behaviors including the number of lanes, length of the speed-change lane, geometry design, signs placement, gaps acceptance and so on [6]–[9]. Laval *et al.* proposed a multilane hybrid model with the speed difference across lanes [10], [11]. Xuan *et al.* proposed a lane-mark extraction algorithm based on computer vision detection technology [12]. Speed, speed difference and density difference are introduced to address the safety effect. Psychological indicators such as eye movement, head movement and electroencephalogram are also used to describe the lane-changing behavior. Yuan *et al.* explored a new identification method for lane changing intention by analyzing eye movement behavior [13], [14]. The electroencephalogram is used to estimate the driver's intention and lane departure [15]–[17]. The driver's head motion is also used to identify the lane changing behaviors [18], [19]. The driver perception characteristics are used to develop a theoretical warning model of lane change [20]. The 3D body posture of the driver is used to study the lane changing behaviors [21], [22]. Vehicle trajectories are collected from vehicles and used to develop the lane-changing behavior [23]. The Next Generation Simulation (NGSIM) trajectory data sets are frequently employed to explore lane-changing behavior. Przybyla *et al.* employed NGSIM to develop a car-following model under natural driving data [24]–[27]. Steering features

The associate editor coordinating the review of this manuscript and approving it for publication was Muhammad Awais Javed.

are extracted from the trajectories and compared with NGSIM to descript the lane-changing behavior [28]–[30].

Various models are developed to improve identification accuracies, such as Hidden Markov Model (HMM), logistic regression model (LR), support vector machine (SVM), and Bayesian model. Li *et al.* built the HMM to identify lane-changing behavior with different variables data [31]–[34]. Puan *et al.* used the support vector machine to model lane-changing using loop detector data [35]–[37]. Balal *et al.* used parameters extracted from the vehicle trajectories data to quantify the risk of a lane-changing event on the freeway [38], [39]. [40], [41] designed an algorithm to identify the lane-changing intent with a Bayesian learning methodology, using trajectories. Reference [42] combined physics- and maneuver-based approaches to analyze the lane-changing scenario, using naturalistic driving data. Recently, deep learning and neural network are applied to identify the lane-changing behavior, revealing the effects of uncertainty factors. Kumar *et al.* established a deep learning with steering signal and vehicle speed to simulate the lane-changing decision process [43], [44]. The improved deep learning model is used to predict the lane-changing behavior with traffic features, vehicle parameters and driver motions [45]. Reference [46] developed the dynamic models fit actual lane-change trajectories better and can generate more accurate lane-change trajectories. Morris *et al.* developed a fuzzy neural network [47].

The current researches have some inadequacies. Some inputs of identification model are hard to be recorded during driving. For example, the collection of visual data and electroencephalogram (EEG) data of driver affects the safety of driving. Unfortunately, some input parameters of identification models are proved to be difficult to quantify, resulting in the low identification accuracy. Some researchers only used vehicle operating parameters or driver psychology indicators, lowering the prediction precision of models. Vehicle trajectories are obtained to model the lane-changing behavior in certain road scenario. Most of the research of lane-changing is on the freeway, only focused on ordinary road sections, and ignore the potentially high risks segments, such as ramps and intersection. Besides, it is time-consuming and expensive to collect massive, natural driving data from real vehicles for lane-changing behavior with these conventional approaches.

It is significantly important to warn the lane-changing of other vehicles in advance. The objective of this paper is to explore features which may be able to identify lane-changing behaviors at off-ramps in the initial stage. This paper collected vehicle trajectories at off-ramps of freeway using an unmanned aerial vehicle (UAV). A hybrid model, combining the Gaussian Mixture Model (GMM) and Continues Hidden Markov Model (CHMM), is proposed to recognize lane changing behavior observed at freeway exits. The remaining part of this paper is organized as follows: Section 2 introduced the video data collection and features extraction process; Section 3 is the establishment of the hybrid model; Section 4 is the model training results for lane-changing and keeping; Section 5 gives the research conclusions.

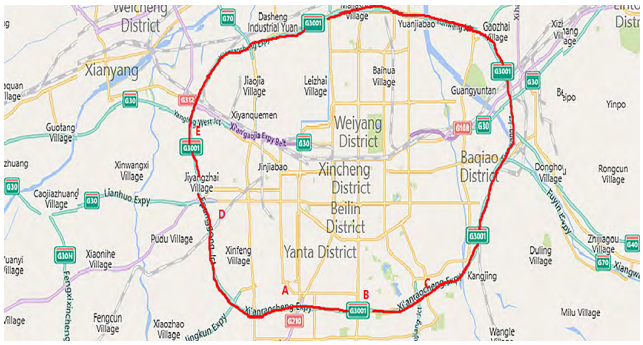

FIGURE 1. The Xi'an Raocheng freeway.

II. DATA ANALYSIS

A. DATA COLLECTION

The video data was recorded from Xi'an Raocheng freeway, which is a six-lane freeway and the lane width is 3.75m. The total length of the road is 33.852 km. The horizontal radius of the road is greater than 600m. The design speed is 120km/h. The speed limit is 120km/h for passenger cars and 80km/h for trucks, respectively. There are 18 interchanges totally, and we selected five with heavy traffic flow for investigation. The road alignment is similar at five sites. The length of the deceleration lane is 240m. The warning signs are placed at 2km, 1km, and 500m, respectively, before exits. The vehicles are divided into passenger cars and trucks, according to ''Technical Standard for Highway Engineering 2016''. Vehicles, of which the axis distance is greater than 3.8m, are trucks. Otherwise, the vehicles are defined as passenger cars.

The video of the traffic flow was captured with the DJY Inspire 2 drone from the manufacturer SZDJI SZ DJI Technology Co., Ltd., and positioned at the five chosen off-ramp interchanges. Four batteries were prepared to support the drone to operate continuously during investigation. The flying altitude of the drone was 150 meters, and the size of the area to be surveyed at each off-ramp was 350×190 m^2. On weekdays from November 5th to November 9th, 2018, we collected video for 20 minutes at each site every day in the morning peak hours (7:00-9:00 am). During the investigation period, the air pollution index (API) was less than 100, and the weather was clear, and visibility was sufficient for HD video. 500 minutes of video was collected. Fig.1 is the investigation locations at Xi'an Raocheng freeway. Fig.2 is the video image collected by UAV.

B. VEHICLE TRAJECTORIES EXTRACTION

The off-ramp influence area in this study is 150m past the ramp and 200m before, and there is no on-ramp in this area. The slope of the road segment is less than 3%. The vehicle trajectories were extracted from the video images at a frequency of 5Hz by the Tracker.

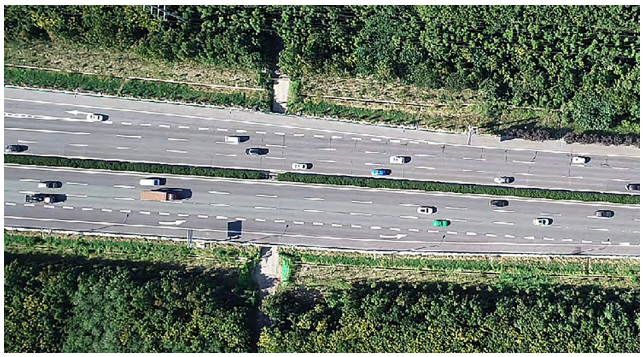

FIGURE 2. The collected video image from UAV.

We used the software Tracker to obtain video trajectories automatically. Tracker is a free video analysis and modeling tool based on the Open Source Physics Java framework, and it consists of a Java™ runtime environment and Xuggle video engine. In our study, we can track the individual vehicle position, velocity, and acceleration speed automatically and manually.

The vehicle extraction process is as follows.

Step 1: Coordination setting. A coordinate reference system is set up in the video image as Fig. 3 to calculate the vehicle positions. In order to utilize the further analysis process, the X-axis is the central line of the outer lane closing to the exit. The Y-axis is perpendicular to the central line of the lane. The right direction is the positive direction of X-axis, and the upward direction is the positive direction of Y-axis.

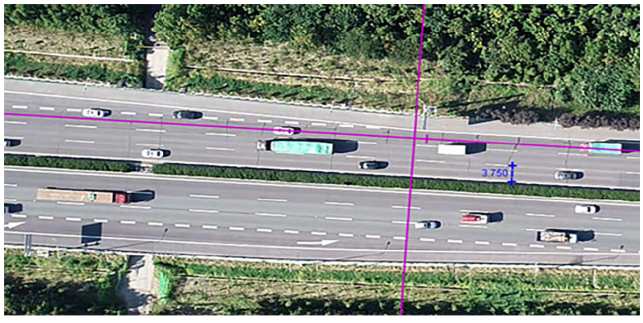

FIGURE 3. The coordinate system in the video image.

Step 2: Calibration. The spatial calibration is required to transform image space proportionately to the ground plane using a standard length. In this study, the 3.75m of lane width is used to calibrate the position of vehicles on the ground.

Step 3: A one-second video is composed of 25 frames. We recorded the positional of vehicles every five frames. A coordinate reference system is set up in the video to calculate positions of vehicles at different times. We set the target vehicle as a template image. The software recorded the features of the target vehicle and tracked it automatically as Fig. 4.

FIGURE 4. The traveling trajectory of vehicles.

The red diamond-shaped points represent the trajectories of the target vehicle in Fig. 4. The section of the vehicle body in the red circle is the template image we set up and it is significantly different from the environment around. Therefore, the vehicle shadow does not affect the extraction of the vehicle trajectory.

Step 4: We calculated parameters for each vehicle. Parameters such as the coordinate's values of X-axis and Y-axis, distance to the origin point, the vehicle speed in space, speed component in X-axis, speed component in Y-axis, acceleration speed in space, acceleration component in X-axis, acceleration component in Y-axis.

Fig. 5 is the position of each vehicle in the longitude direction. In Fig. 5, t is the sampling time interval, and x is the value of X-axis in the image, which multiple 100m is the real distance. The speed component in X-axis is calculated from the line. In Fig. 6, t is the sampling time and y is the value of Y-axis in the image, which multiple 100m is the real distance. The speed component in Y-axis is calculated from the line.

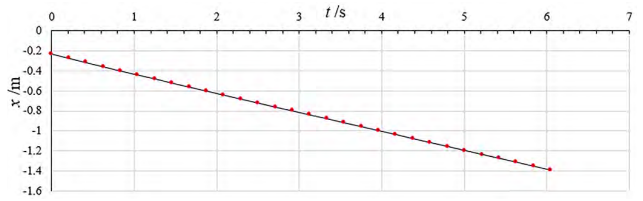

FIGURE 5. The vehicle position at the longitude direction.

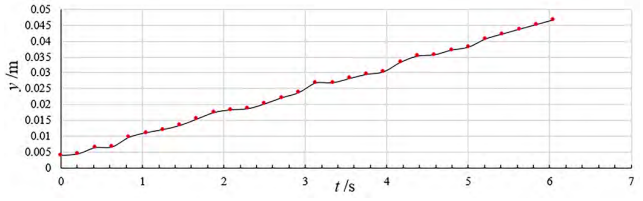

FIGURE 6. The vehicle position at the lateral direction.

C. TRAFFIC FLOW COLLECTION

The images of video demonstrate that 17% of the vehicles enter the off-ramp after a lane-changing behavior. The drone also flies down 44m to collect the traffic flow features in

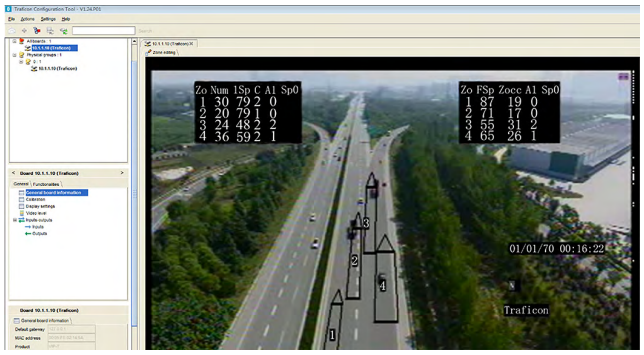

FIGURE 7. The automatic detection of Flux.

this experiment. Four virtual loops have been placed in the target lanes as Fig. 7. The vehicles with length more than 6m are defined as trucks. The features such as traffic volume, mean speed and traffic density were calculated automatically for mainline by software Flux. Then we obtain truck percentage manually. Records of any vehicle speeds over 120km/h are eliminated. The summary of traffic features is as Table. 1.

TABLE 1. Traffic flow statistics at five sites.

Site	Traffic volume (pcu/h)	85% speed (km/h)	Mean speed (km/h)	Traffic density (pcu/km)	Truck percentage
A	3733	94.53	78.55	17.4	22.6%
B	3912	92.21	77.23	17.6	21.5%
C	3545	91.87	76.66	17.8	26.1%
D	4626	93.56	77.65	17.5	23.8%
E	3865	90.21	77.34	17.7	21.8%

Table. 1 is the traffic flow statistics of Xi'an Raocheng freeway. The traffic flow is between 3500 pcu/h∼4700 pcu/h. The 85% speed is above 90km/h and the mean speed is 77km/h. The truck percentage is around 20% percentage, which shows that the prevailing vehicle type is the passenger car for this freeway.

D. FEATURE EXTRACTION

We divide drivers' behaviors into lane-changing and lane-keeping. It is found that the lane-changing behavior lasts six seconds for analyzing the recorded data. Therefore, we preferred 6 seconds window to identify lane-changing and keeping behavior. A one-second record consists of 25 frames in this study. We recorded parameters of one point every five frames. Five records of each parameter are extracted, respectively, per second and therefore, we obtained 30 records for each trajectory sample. Finally, we extracted 205500 records, consisting of 3410 samples of lane-changing and 3440 keeping samples at freeway exits.

Correctness is a characteristics index, and it is one of the most important measurements for the quality of data. The correctness can be measured as (1):

$$Q_c = 1 - \frac{\text{The number of incorrect data records}}{\text{Total number of incorrect data records}}, \quad (1)$$

In order to evaluate the quality of the driving trajectory data we extracted from the video stream, 50 samples were randomly selected from all trajectory samples, because the characteristics of the subsample set can represent the whole.

In this study, Grubbs outlier test is used to distinguish the outliers of the original data based on the speed of each sample point of each trajectory as (2). The outliers were treated as incorrect data records, and replaced by the mean of the adjacent points. Then correctness is calculated to evaluate the data based on the number of outliers.

$$G_j = \frac{|v - \overline{v}|}{S} \geq G(p, n), \quad (2)$$

where G_j denotes Grubbs' test statistic. v denotes the speed of each sample calculated from one trajectory. $\overline{v}$ denotes the mean of speed from one trajectory sample. S denotes the standard deviation of speed from one trajectory sample. $G(p, n)$ denotes Grubbs' critical value. p denotes confidence interval and generally, p is set to 0.95. n denotes the number of records of each sample and it is 30 in the study. The value of $G(0.95, 30)$ is 2.745, found from the table of critical values for Grubbs' test.

The correctness of each sample is calculated as (3) :

$$Q_c = 1 - \frac{\text{The number of outlier}}{30}, \quad (3)$$

Therefore, the correctness of the subsample is calculated as the following:

$$\mathrm{Q_c} = \frac{1}{50}\sum_{\mathrm{c}=1}^{50} \mathrm{Q_c} = 98.47\%$$

The correctness of the total sample is 98.47%. It shows that the quality of data we extracted is high enough for modeling.

Finally, we collected 205500 records including 3410 trajectory samples of lane-changing (L-C) and 3440 trajectory samples of lane-keeping (L-K). Features such as lane departure value, speed, acceleration speed, angle between moving direction and X-axis, angle between r and Y-axis are summarized as Table. 2. Each parameter is interpreted as Fig. 8.

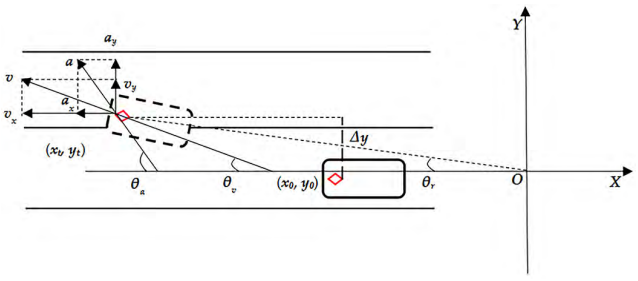

FIGURE 8. The demonstration of each parameter.

Table. 2 shows that the parameters such as lateral driving speed, lane departure, and the lane deviation angle can be used to explain lane-changing behavior at the freeway off-ramps. Therefore, we use the vector $(\Delta y, v_y, \theta_v)$ as a feature vector to develop identification model of trajectories.

TABLE 2. The parameters statistics.

Parameters	Interpretation	Behavior	N	Mean	Std. Dev
Δy	lane departure(m)	L-C	3410	1.10	0.76
		L-K	3440	-0.15	0.13
v_x	horizontal speed(m/s)	L-C	3410	-18.18	0.29
		L-K	3440	-16.88	0.25
v_y	vertical speed(m/s)	L-C	3410	0.54	0.37
		L-K	3440	-0.05	0.15
v	vehicles speed in space(m/s)	L-C	3410	18.19	0.29
		L-K	3440	16.89	0.25
a_x	horizontal acceleration(m/s²)	L-C	3410	0.07	0.83
		L-K	3440	0.01	0.80
a_y	vertical acceleration(m/s²)	L-C	3410	0.19	0.99
		L-K	3440	-0.05	0.55
a	acceleration in space(m/s²)	L-C	3410	1.07	0.72
		L-K	3440	0.72	0.64
θ_r	angle between r and lane line(°)	L-C	3410	2.99	0.55
		L-K	3440	0.47	0.98
θ_v	lane deflection angle(°)	L-C	3410	2.02	0.78
		L-K	3440	0.36	0.37
θ_a	acceleration deflection angle(°)	L-C	3410	9.95	51.86
		L-K	3440	16.35	47.18

The independent T-test is a statistical test, which determines whether there is a statistically significant difference between the means in the above two unrelated groups, for the same continuous and dependent variable. Table. 3 is the independent test samples results.

TABLE 3. Independent samples test.

		Test for Variances		T-test for Equality of Mean
		F	Sig	Sig. (2-tailed)
Δy	equal variances assumed	38.431	0.000	0.000
	Equal variances not assumed			0.000
v_y	equal variances assumed	11.851	0.001	0.000
	Equal variances not assumed			0.000
θ_v	equal variances assumed	5.840	0.019	0.000
	Equal variances not assumed			0.000

Table. 3 shows that there are only three variables significant which can represent the driving behaviors including $\Delta \boldsymbol{y}$,$\boldsymbol{v_y}$, and $\boldsymbol{\theta_v}$.Δy in Table. 3 denotes lane departure as (4). $\Delta\ y_t$ means lane departure at time t. y_t means coordinate of Y-axis at time t and y_0 means coordinate of Y-axis at time 0.

$$\Delta y_t = y_t - y_0, \tag{4}$$

In Table. 3, the lateral driving speed of the vehicle, lane departure, and lane deviation angle are with a statistically significant difference between the means in lane-changing and keeping. As shown in Table. 2, the mean values of driving lateral speed for lane-changing and keeping are 0.54 m/s and -0.05 m/s respectively. The mean values of lane departure for lane-changing and keeping are 1.10 m and -0.15 m respectively. The mean values of lane deviation angle for lane-changing and keeping are 2.02° and 0.36° respectively.

III. METHODOLOGY

In this paper we established a hybrid model to identify and predict lane-changing behavior at the freeway off-ramps. It is important to recognize driving behavior in the initial stage, which can be implemented by continuous recognition. Therefore, CHMM is employed in this study.

A. GAUSSIAN MIXTURE MODEL

GMM is employed to describe the probability distribution of all continuous variables we extracted and describe the correlation between every two different variables. The GMM consists of K Gaussian models as (5).

$$G(x) = \sum_{k=1}^{K} C_k g(x; \mu_k, \Sigma_k), \tag{5}$$

where $g(x; \mu_k, \Sigma_k)$ indicates the k^{th} sub-Gaussian model. The probability density function of the Gaussian model is shown as (6). $\boldsymbol{x}$ is the lane-changing samples for training and it consists of d continuous variables. The value of C_k denotes the weight of the k^{th} sub-Gaussian model, and they are related to the composition of $\boldsymbol{x}$. $\mu_{\mathbf{k}}$ and $\Sigma_{\mathbf{k}}$ are the mean matrix and covariance matrix of all the continuous variables in the k^{th} sub-Gaussian model, respectively.

$$g(x; \mu, \Sigma) = \frac{1}{\sqrt{(2\pi)^d |\Sigma|}} \exp\left[-\frac{1}{2}(x-\mu)^T \Sigma^{-1}(x-\mu)\right], \tag{6}$$

In order to get all the parameters of GMM from lane-changing samples, the Maximum Likelihood Estimation and the Expectation-Maximization algorithm (E-M) can be combined.

Because the probability of each sample generated by GMM is very small, we use the log-likelihood function as (7).

$$p(x|C_k, \mu_k, \Sigma_k) = \sum_{i=1}^{N} \log\left\{\sum_{k=1}^{K} C_k g(x_i; \mu_k, \Sigma_k)\right\}, \tag{7}$$

$p(x|C_k, \mu_k, \Sigma_k)$ denotes the probability of all the sample points generated by the GMM. Generally, we get the last parameters when $p(x|C_k, \mu_k, \Sigma_k)$ reaches a maximum.

The Expectation-Maximization (E-M) algorithm consists of an E-step and an M-step. Expectation step is to calculate the expectation $\varphi(i, k)$ as (8).

$$\varphi(i, k) = \frac{C_k g(x; \mu_k, \Sigma_k)}{\sum_{k=1}^{K} C_k g(x; \mu_k, \Sigma_k)}, \tag{8}$$

where $\varphi(i, k)$ denotes the probability of the k^{th} sub-Gaussian model generating the i^{th} lane-changing sample point.

The M step is to recalculate C_k, μ_k and Σ_k based on $\varphi(i, k)$. The iterating E and M step stop until the log-likelihood converges.

B. CONTINUOUS HIDDEN MARKOV MODEL

A Hidden Markov Model is a stochastic model consisting of a Markov chain and stochastic process for hidden state prediction. In this study, the hidden states are lane-changing and lane-keeping. Each hidden state cannot be observed, but it can generate observation vectors, consisting of several variables. In this study, these variables are lateral driving speed, lane departure, and the lane deviation angle. Fig. 9 shows the Markov process.

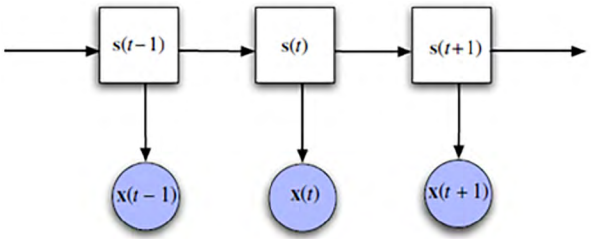

FIGURE 9. Markov process.

In Fig. 9, $s(t-1)$,$s(t)$ and $s(t+1)$ denotes the hidden state at time $t-1$, t and $t+1$, respectively. The probability of a hidden state in current moment only depends on the previous hidden state: $p(s(t)|s(t-1)\ldots s(1)) = p(s(t)|s(t-1))$.$x(t-1)$, $x(t)$ and $x(t+1)$ denotes the observation vector at time $t-1$, t and $t+1$, respectively and the probability of an observation vector only depends on the hidden state generated by $p(x(t)|s(t-1)\ldots s(1), x(t-1)\ldots x(1) = p(x(t)|s(t))$.

Because of the variables extracted from images are continuous numerical variables, the common basic HMM is suitable for discrete variables. Then we choose the Continuous Hidden Markov Model (CHMM) to identify driver behaviors.

A basic HMM consists of three parameters: $\boldsymbol{\pi}, \boldsymbol{A}, \boldsymbol{B}$. $\boldsymbol{\pi}$ is the hidden state probability distribution at the initial time. $\boldsymbol{A}$ is the state transition probability matrix, which is made up of the transition probability between different hidden states, such as the lane-changing state and lane-keeping state. $\boldsymbol{B}$ is the observation probability matrix, which is made up of the probability that the observation vector observed at each hidden state. In a CHMM, parameter $\boldsymbol{B}$ has some changes that $\boldsymbol{B}$ is divided into three parts, and they are $\boldsymbol{C}$, $\boldsymbol{\mu}$, and $\boldsymbol{\Sigma}$. They are generated by GMM as (9)∼(10). Therefore the general model of CHMM is $\boldsymbol{\lambda} = (\boldsymbol{\pi}, \boldsymbol{A}, \boldsymbol{C}, \boldsymbol{\mu}, \boldsymbol{\Sigma})$.

$$b_j(O_t) = \sum_{k=1}^{K} C_{jk}\, g\left(O_t; \mu_{jk}, \Sigma_{jk}\right) = \sum_{k=1}^{K} C_{jk} b_{jk}(O_t), \quad (9)$$

$$g\left(O_t; \mu_{jk}, \Sigma_{jk}\right) = \frac{1}{\sqrt{(2\pi)^d |\Sigma_{jk}|}} \exp\left[-\frac{1}{2}\left(O_t - \mu_{jk}\right)^T \Sigma_{jk}^{-1}\left(O_t - \mu_{jk}\right)\right], \quad (10)$$

where $b_j(O_t)$ denotes the probability of the observation vector $\boldsymbol{O_t}$ generated by state j. $\mathbf{g}$ is the k^{th} sub Gaussian model of GMM. The GMM is used to describe the probability distribution of three continuous variables and we can get the probability of any observation vector made up of these three continuous variables by putting them into GMM. C_{jk} is the weight value of the k^{th} sub-Gaussian model at hidden state j. $\boldsymbol{\mu_{jk}}$ is the mean matrix of the k^{th} sub Gaussian model at hidden state j, $\boldsymbol{\Sigma_{jk}}$ is the covariance matrix of the k^{th} sub-Gaussian model at hidden state j.

In order to estimate the parameters $\boldsymbol{\pi}$, $\boldsymbol{A}$, $\boldsymbol{C}$, $\boldsymbol{\mu}$, and $\boldsymbol{\Sigma}$, the Baum-Welch algorithm has been applied. It combines the Forward algorithm, Backward algorithm and the E-M algorithm together. The Forward algorithm is used to calculate the forward variable that is indicated by $\alpha_t(i)$ as (11)∼(12) and it is the joint probability of the partial observation sequence $(O_\tau, \tau = 1, 2\ldots t)$, consisting of t observation vectors, besides given that the hidden state is i at time t.

$$\alpha_t(i) = p\{(O_1\ldots O_t, s_t = i)|\lambda = (\pi, A, C, \mu, \Sigma)\}, \quad (11)$$

$$\alpha_t(i) = \left[\sum_{j=1}^{N} \alpha_{t-1}(j)\, a_{ij}\right] b_i(o_t), \quad (12)$$

The Backward algorithm is used to calculate the backward variable that is indicated by $\beta_t(i)$ as (13)∼(14) and it is the joint probability of the partial observation sequence $(O_\tau, \tau = t+1, t+2\ldots$, consisting of T-t observation vectors, besides given that the hidden state is i at time t.

$$\beta_t(i) = p\{(O_{t+1}\ldots O_T, s_t = i)|\lambda = (\pi, A, C, \mu, \Sigma)\}, \quad (13)$$

$$\beta_t(i) = \sum_{j=1}^{N} a_{ij} b_j(o_{t+1})\, \beta_{t+1}(j), \quad (14)$$

The E-M algorithm is used to iteratively recalculate the parameters and we obtain a maximum likelihood estimate of the CHMM. By dividing likelihood estimate function $p(O|\lambda)$ into five parts, we can get the formats of $\boldsymbol{\pi}$, $\boldsymbol{A}$, $\boldsymbol{C}$, $\boldsymbol{\mu}$, and $\boldsymbol{\Sigma}$ respectively and $p(O|\lambda)$ is the conditional probability of the entire observation sequence OO generated by the model.

The E-M algorithm consists of the Expectation step and the Maximization step. The E step is used in estimation of two probability variables $\gamma_t(i)$, $\xi_t(i,j)$ as (14)∼(15) and initialize the values of $\boldsymbol{\pi}$, $\boldsymbol{A}$, $\boldsymbol{C}$, $\boldsymbol{\mu}$, and $\boldsymbol{\Sigma}$. The M step is to re-estimate them based on $\gamma_t(i)$, $\xi_t(i,j)$, until they all reach convergence.

$$\gamma_t(i) = \frac{\alpha_t(i)\,\beta_t(i)}{\sum_{i=1}^{N} \alpha_t(i)\,\beta_t(i)}, \quad (15)$$

$$\xi_t(i,j) = \frac{\alpha_t(i)\, a_{ij} b_j(o_{t+1})\, \beta_{t+1}(j)}{\sum_{I=1}^{N}\sum_{j=1}^{N} \alpha_t(i)\, a_{ij} b_j(o_{t+1})\, \beta_{t+1}(j)}, \quad (16)$$

where $\gamma_t(i)$ is the probability that the hidden state is i at time t, besides given the observation sequences $\boldsymbol{O}$. $\xi_t(i,j)$ is the probability that the hidden states are i and j at time t and $t+1$, respectively, besides given the observation sequences $\boldsymbol{O}$.

IV. LANE-CHANGING MODEL

A. MODEL TRAINING

In our study, lane-changing detection and identification are achieved in a continuous manner. In a continuous identifier, each complete maneuver is modeled as a Markov model. The general model of the CHMM is $\lambda = (\boldsymbol{\pi}, \boldsymbol{A}, \boldsymbol{C}, \boldsymbol{\mu}, \boldsymbol{\Sigma})$.

λ_C and λ_K has been trained by a set of trajectory samples for the complete lane-changing maneuver and lane-keeping maneuver, respectively.

In this training step, all the trajectories samples we recorded at freeway off-ramps are classified into lane-changing and keeping behavior. Each trajectory sample consists of 30 records and each record is just a feature vector, consisting of lateral driving speed, lane departure and the lane deviation angle. Each feature vector may be generated by the different hidden states, and the hidden states are the lane-changing and lane-keeping. Each lane-changing or keeping driving trajectory consists of 30 feature vectors and each vector is generated by lane-changing or lane-keeping hidden state.

In order to identify lane-changing behavior, λ_C and λ_K are trained, respectively. We trained λ_C and λ_K based on lane-changing trajectory samples and lane-keeping trajectory samples respectively. Training λ_C contains the following three steps.

Step 1: Initialization. Before iterating to determine all the parameters of λ_C, it is necessary to initialize all the parameters and they are K, $\boldsymbol{\pi}$, $\boldsymbol{A}$, $\boldsymbol{C}$, $\boldsymbol{\mu}$, and $\boldsymbol{\Sigma}$. The GMM is the most classical method to extract the image from the background and basically 3 to 5 Gaussian models making up GMM to characterize the features of each pixel in the image. Therefore, in order to simplify the model, we set the initial value of K to 3. Because we chose lane-changing trajectory to train λ_C, it is logical to consider that the initial hidden state is the same as the last state and it is a lane-keeping state. Therefore, the initial lane-changing state probability is set to zero and lane-keeping state probability is set to one, respectively. We gave $\boldsymbol{A}$, $\boldsymbol{C}$, $\boldsymbol{\mu}$, and $\boldsymbol{\Sigma}$ initial values randomly at the same time.

Step 2: Determining lane-changing trajectory samples as observation sequence $\boldsymbol{O_\tau}$. Each sequence is a trajectory sample consisting of 30 feature vectors, and these feature vectors are in order. We randomly chose 66% of the lane-changing trajectory samples being set as the model training set (2251 samples) and the remaining 34% was set as a test set (1159 samples) based on the Holdout cross-validation method. Table. 4 presents the partial lane-changing trajectory sample records.

Step 3: Iterative optimization. The input of iteration is initial values containing $\boldsymbol{\pi}$, $\boldsymbol{A}$, $\boldsymbol{C}$, $\boldsymbol{\mu}$, $\boldsymbol{\Sigma}$ and the observation sequence $\boldsymbol{O_\tau}$ consisting of lateral driving speed of vehicle v_y, lane departure Δy and speed deflection angle θ_v. The identification model is the CHMM mixed with the GMM. The observation probability matrix $\boldsymbol{B}$ consists of $\boldsymbol{C}$, $\boldsymbol{\mu}$, $\boldsymbol{\Sigma}$, and they are generated by the GMM. Two identification models are lane-changing and lane-keeping. Each identification model contains six Gaussian models belonging to two GMM and each GMM has three.

Under the MATLAB 2014Ra platform, we utilized these steps based on the Baum-Welch algorithm. Finally, the log-likelihood converges in forty-one iterations as Fig. 10. And we obtained the lane-changing identification model λ_C.

TABLE 4. The training set samples.

No.	Sample time(s)	Lane departure (m)	Lateral driving speed (m/s)	Lane deflection angle (°)
1	0	0	0.144	1.1
2	0.209	0.067	0.342	1.7
3	0.417	0.142	0.563	2.3
4	0.626	0.302	0.353	2.2
5	0.834	0.29	0.353	1.1
6	1.043	0.449	0.615	0.1
7	1.251	0.546	0.463	2.2
8	1.460	0.643	0.480	3.3
9	1.669	0.746	0.235	1.2
10	1.877	0.741	0.362	2.2
11	2.086	0.897	0.488	2.3
12	2.294	0.944	0.117	1.8
13	2.503	0.946	0.218	1.8
14	2.711	1.035	0.48	2.2
15	2.92	1.146	0.775	3.0
16	3.128	1.359	0.488	1.7
17	3.545	1.344	0.636	2.5
18	3.754	1.615	1.108	1.6
19	3.963	1.806	0.413	1.4
20	4.171	1.787	0.246	1.7

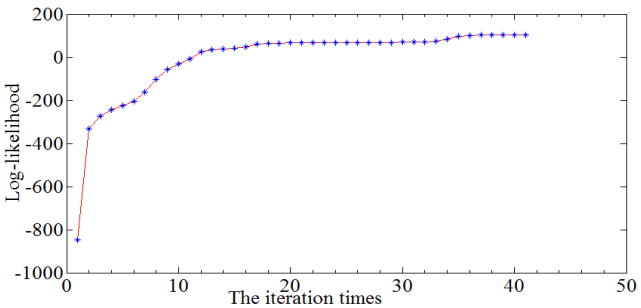

FIGURE 10. The iterative procedure.

λ_c is made up of $\boldsymbol{\pi}$, $\boldsymbol{A}$, $\boldsymbol{C}$, $\boldsymbol{\mu}$, and $\boldsymbol{\Sigma}$ as follows.

$$\boldsymbol{\pi} = \begin{bmatrix} 1 \\ 0 \end{bmatrix},$$

Matrix $\boldsymbol{\pi}$ indicates that the probability of the initial hidden state of lane-changing is zero and lane-keeping is one.

$$\boldsymbol{A} = \begin{bmatrix} 0.8632 & 0.1368 \\ 0.1715 & 0.8285 \end{bmatrix},$$

Matrix $\boldsymbol{A}$ is the probability transition matrix. The transition probability from the current lane-changing to the next lane-changing state is 0.8632. The transition probability from the current lane-changing to the next lane-keeping is 0.1368. The transition probability from the current lane-keeping state to the next lane-keeping is 0.8285. The transition probability from the current lane-keeping to the next lane-changing is 0.1715.

$$\boldsymbol{C} = \begin{bmatrix} 0.4785 & 0.2399 & 0.2816 \\ 0.4871 & 0.3430 & 0.1699 \end{bmatrix},$$

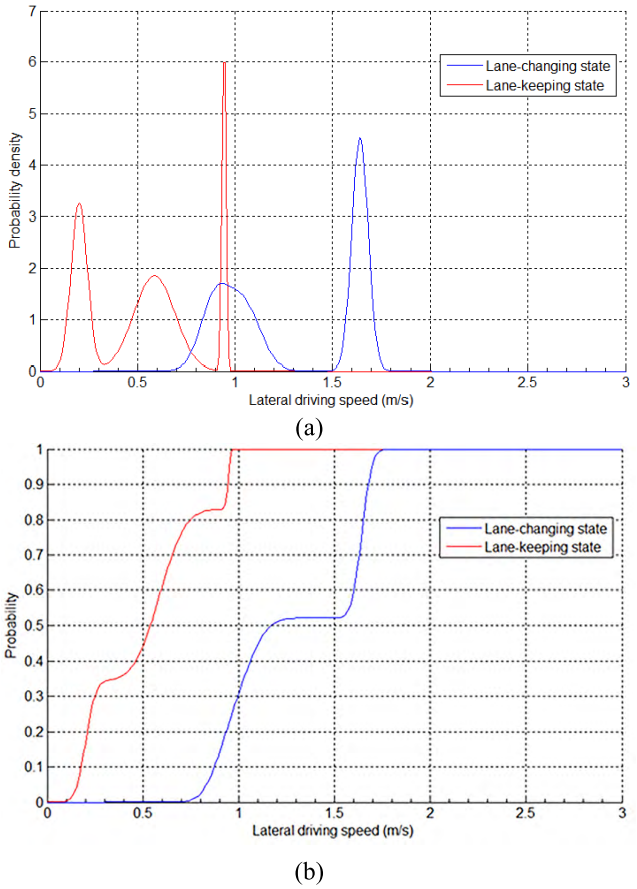

FIGURE 11. The probability density distribution of lateral speed; (a) is the probability density distribution of lateral speed; (b) is the probability cumulative distribution of lateral speed.

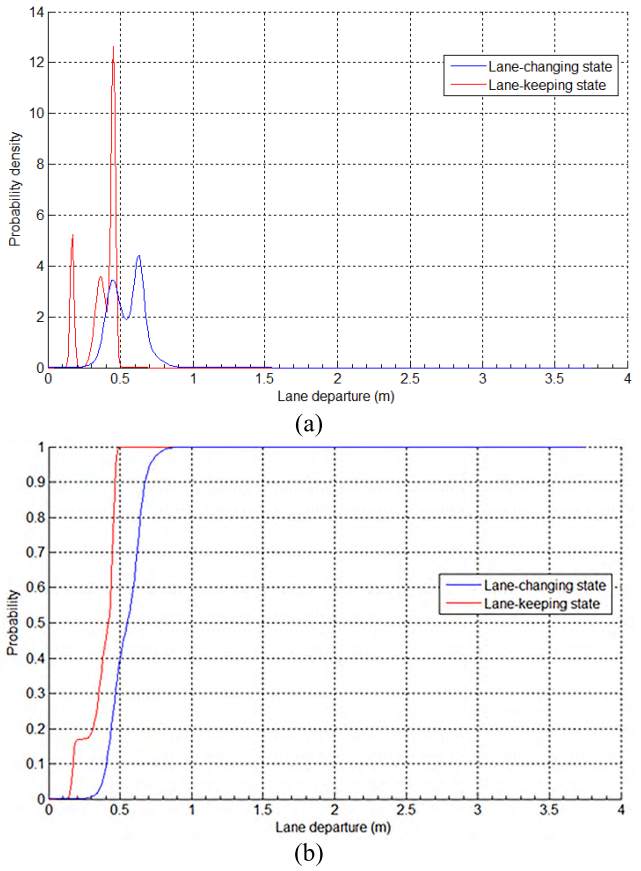

FIGURE 12. The probability density distribution of lane departure; (a) is the probability density distribution of lane departure; (b) is the probability cumulative distribution of lane departure.

The first row of matrix $\boldsymbol{C}$ indicates the weights for the three Gaussian models in the lane-changing state. The second row indicates the weights for the three Gaussian models in the lane-keeping state.

$$\boldsymbol{\mu}(:,:,1) = \begin{bmatrix} 1.6428 & 0.5876 \\ 0.5640 & 0.4500 \\ 2.5996 & 0.2351 \end{bmatrix},$$

$$\boldsymbol{\mu}(:,:,2) = \begin{bmatrix} 0.8943 & 0.2015 \\ 0.6274 & 0.3636 \\ 2.1501 & 0.5011 \end{bmatrix},$$

$$\boldsymbol{\mu}(:,:,3) = \begin{bmatrix} 1.0449 & 0.9450 \\ 0.4404 & 0.1671 \\ 1.8961 & 0.6000 \end{bmatrix},$$

$$\boldsymbol{\Sigma}(:,:,1,1) = \begin{bmatrix} 0.0420 & -0.0161 & 0.0116 \\ -0.0161 & 0.1168 & 0.0023 \\ 0.0116 & 0.0023 & 0.0250 \end{bmatrix},$$

$$\boldsymbol{\Sigma}(:,:,2,1) = \begin{bmatrix} 0.1048 & -0.0028 & 0.0024 \\ -0.0028 & 0.0157 & -0.0027 \\ 0.0024 & -0.0027 & 0.0123 \end{bmatrix},$$

$$\boldsymbol{\Sigma}(:,:,1,2) = \begin{bmatrix} 0.0733 & 0.0371 & 0.0377 \\ 0.0371 & 0.0318 & 0.0221 \\ 0.0377 & 0.0221 & 0.0325 \end{bmatrix},$$

$$\boldsymbol{\Sigma}(:,:,2,2) = \begin{bmatrix} 0.0419 & 0.0271 & 0.0819 \\ 0.0271 & 0.0380 & 0.0660 \\ 0.0819 & 0.0660 & 0.3411 \end{bmatrix},$$

$$\boldsymbol{\Sigma}(:,:,1,3) = \begin{bmatrix} 0.0870 & 0.0514 & -0.1651 \\ 0.0514 & 0.0450 & -0.1133 \\ -0.1651 & -0.1133 & 0.3858 \end{bmatrix},$$

$$\boldsymbol{\Sigma}(:,:,2,3) = \begin{bmatrix} 0.0100 & 0.0001 & 0.0001 \\ 0.0001 & 0.0126 & -0.0001 \\ 0.0001 & -0.0001 & 0.0100 \end{bmatrix},$$

The first column of $\boldsymbol{\mu}(:,:,m)$ indicates the mean value of vector $(\Delta y,\ v_y,\ \theta_v)$ of the m^{th} Gaussian model in the lane-changing state. The second column of $\boldsymbol{\mu}(:,:,m)$ indicates the mean value of vector $(\Delta y,\ v_y,\ \theta_v)$ of the m^{th} Gaussian model in the lane-keeping state.

B. THE DISTRIBUTION FEATURE OF VARIABLES

According to the lane-changing model $\lambda_{\mathbf{C}}$ we trained, we can extract the probability density and probability distribution of every continuous variable in lane-changing hidden state and in the lane-keeping state. They show the individual features of lane-changing behavior different from lane-keeping as Fig. 11-13.

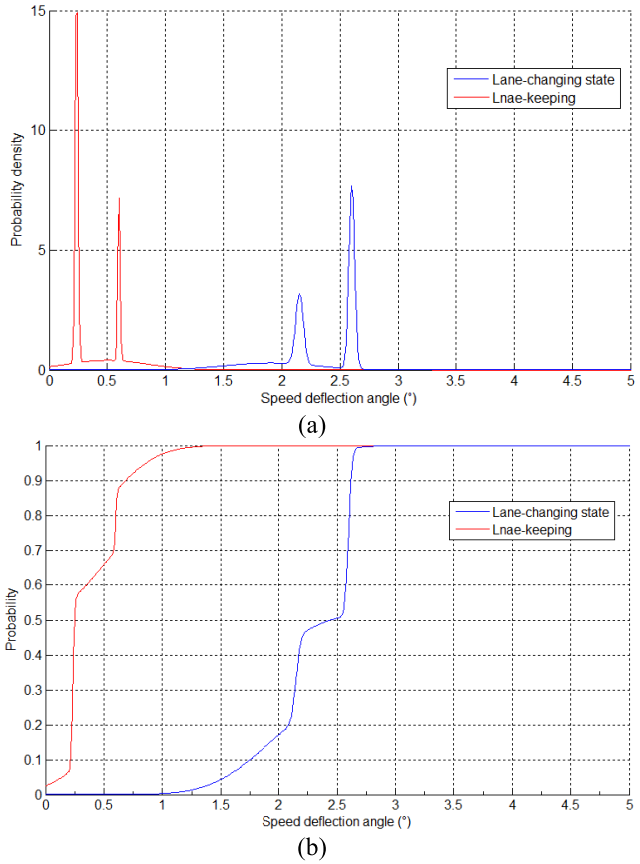

FIGURE 13. The probability density and distribution of lane deviation angle; (a) is the probability density for the lane deviation angle;(b) is the cumulative probability distribution of lane deviation angle.

Fig. 11 shows that the lateral speed of lane-changing mainly distributes in the range of (1, 2), and distributes in the range of (0,1) of lane-keeping.

Fig.12 shows that the lane departure of lane-changing mainly distributes in the range of (0.5, 1). And it mainly distributes in the range of (0, 0.5) of lane keeping.

Fig. 13 shows that the lane deviation angle of lane-changing mainly distributes in the range of (1, 2.6), and mainly distributes in the range of (0, 1) of lane keeping.

They show that there are obvious distinctions in the distribution of lateral driving speed, lane departure, and speed deflection angle between lane-changing and lane-keeping behavior. It proves that it is reasonable to set these three variables as the feature of lane-changing behavior.

C. LANE CHANGE PREDICTION

The workflow of predicting lane-changing and lane-keeping is shown in Fig. 14. The trajectory samples extracted from the traffic flow is processed and set as an observation sequence $\boldsymbol{O_\tau}$. $\boldsymbol{O_\tau}$ is the input of $\boldsymbol{\lambda_C}$ and $\boldsymbol{\lambda_K}$. Then $p(\boldsymbol{O_\tau}|\,\boldsymbol{\lambda_C})$ and $p(\boldsymbol{O_\tau}|\,\boldsymbol{\lambda_K})$ is calculated for prediction.

In order to test the accuracy of predicting the driving behavior of $\boldsymbol{\lambda_C}$ and $\boldsymbol{\lambda_K}$ we trained, 34% trajectory samples we collected were considered as a test set based on the Hold-out cross-validation method. 1159 lane-changing trajectory samples and 1170 lane-keeping trajectory samples are set as a test set to validate the driving state of each sample. Table. 5 presents the partial test results.

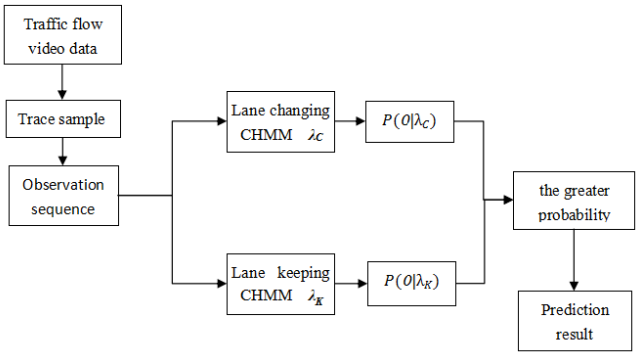

FIGURE 14. The workflow of prediction.

TABLE 5. Lane change prediction.

Sample No.	λ_C	λ_K	Prediction result
1	-75.23	-202.36	Lane-changing
2	-56.54	-196.56	Lane-changing
3	-137.25	-82.53	Lane-keeping
4	-84.52	-162.35	Lane-changing
5	-59.21	-138.57	Lane-changing
6	-49.87	-123.98	Lane-changing

TABLE 6. The accuracy of testing.

	Lane-changing trajectory	Lane-keeping trajectory
Testing samples	1159	1170
Correct identifications	1094	1095
Accuracy	94.4%	93.6%

Table. 6 shows the accuracy of predicting lane-changing and lane-keeping behavior at the freeway off-ramps, by the proposed model. The accuracy of predicting the lane-changing behavior is 94.4%. The accuracy of predicting the lane-keeping behavior is 93.6%.

V. CONCLUSIONS

The paper presents a hybrid model for the lane-changing prediction at freeway off-ramps. We collected 205500 trajectory records at five investigation sites. The experiment draws the following conclusions.

(1) The parameters such as lateral driving speed, lane departure and the lane deviation angle obtained from the driving trajectories can be applied to explain the lane-changing behavior at freeway off-ramps.

(2) The identification models can achieve 94.4% accuracy for lane-changing and 93.6% for lane-keeping.

(3) The trained models can predict driving behaviors without additional sensors on the vehicle. It can be integrated into traffic cameras to detect the unsafe driving behavior and give warning to drivers.

REFERENCES

[1] T. M. A. Bureau, "Road accidents statistical annual report 2016," Ministry Public Secur. China, Beijing, China, Tech. Rep., Jul. 2017.

[2] J. Li-Sheng, F. Wen-Ping, Z. Ying-Nan, Y. Shuang-Bin, and H. Hai-Jing, "Research on safety lane change model of driver assistant system on highway," in *Proc. IEEE Intell. Vehicles Symp.*, Xi'an, China, Jun. 2009, pp. 1051–1056.

[3] S. Yim and Y. Park, "Design of rollover prevention controller with linear matrix inequality-based trajectory sensitivity minimisation," *Vehicle Syst. Dyn.*, vol. 49, no. 8, pp. 1224–1225, Aug. 2011.

[4] A. T. McCartt, V. S. Northrup, and R. A. Retting, "Types and characteristics of ramp-related motor vehicle crashes on urban interstate roadways in Northern Virginia," *J. Saf. Res.*, vol. 35, no. 1, pp. 107–114, 2004.

[5] C. Ma, W. Hao, W. Xiang, and W. Yan, "The impact of aggressive driving behavior on driver-injury severity at highway-rail grade crossings accidents," *J. Adv. Transp.*, vol. 2018, no. 58, Oct. 2018, Art. no. 9841498.

[6] H. Chen, H. Zhou, and P.-S. Lin, "Freeway deceleration lane lengths effects on traffic safety and operation," *Saf. Sci.*, vol. 64, pp. 39–49, Apr. 2014.

[7] M. Zahabi, P. Machado, M. Y. Lau, Y. Deng, C. Pankok, Jr., J. Hummer, W. Rasdorf, and D. B. Kaber, "Driver performance and attention allocation in use of logo signs on freeway exit ramps," *Appl. Ergonom.*, vol. 65, pp. 70–80, Nov. 2017.

[8] H.-J. Zhao and H.-P. Zhao, "Geometric safety design of freeway off-ramp-street terminal based on traffic flow characteristic analysis," in *Green Intelligent Transportation Systems-GITSS* (Lecture Notes in Electrical Engineering), vol. 419. Singapore: Springer, 2017, pp. 1023–1034.

[9] M. Sarhan, Y. Hassan, and A. O. A. El Halim, "Safety performance of freeway sections and relation to length of speed-change lanes," *Can. J. Civil Eng.*, vol. 35, no. 5, pp. 531–541, May 2008.

[10] J. A. Laval and L. Leclercq, "Microscopic modeling of the relaxation phenomenon using a macroscopic lane-changing model," *Transp. Res. B, Methodol.*, vol. 42, no. 6, pp. 511–522, Jul. 2008.

[11] F. Chen, S. Chen, and X. Ma, "Analysis of hourly crash likelihood using unbalanced panel data mixed logit model and real-time driving environmental big data," *J. Saf. Res.*, vol. 65, pp. 153–159, Jun. 2018.

[12] H. Xuan, H. Liu, J. Yuan, and Q. Li, "Robust lane-mark extraction for autonomous driving under complex real conditions," *IEEE Access*, vol. 6, pp. 5749–5765, 2018.

[13] W. Yuan, R. Fu, F. Wu, and J. Peng, "Analysis of eye movements difference between lane keeping and lane changing intention stage," *J. Chang'an Univ.*, vol. 33, no. 4, pp. 86–91, 2013.

[14] W. Yuan, R. Fu, Y. Guo, J. Peng, and Y. Ma, "Drivers' lane changing intention identification based on visual characteristics," *China J. Highway Transp.*, vol. 26, no. 4, pp. 132–138, 2013.

[15] T. Ikenishi and T. Kamada, "Estimation of driver's steering direction about lane change maneuver at the preceding car avoidance by brain source current estimation method," in *Proc. IEEE Int. Conf. Syst., Man, Cybern.*, San Diego, CA, USA, Oct. 2014, pp. 2808–2814.

[16] C.-T. Lin, J.-T. King, A. K. Singh, A. Gupta, Z. Ma, J.-W. Lin, A. M. C. Machado, A. Appaji, and M. Prasad, "Voice navigation effects on real-world lane change driving analysis using an electroencephalogram," *IEEE Access*, vol. 6, pp. 26483–26492, 2018.

[17] C. Ahlstrom, S. Jansson, and A. Anund, "Local changes in the wake electroencephalogram precedes lane departures," *J. Sleep Res.*, vol. 26, no. 6, pp. 816–819, Dec. 2017.

[18] S. Bi, D. Mei, Z. Liu, and P. Wang, "Research on lane change intention identification model for driving behavior warning," *China Saf. Sci. J.*, vol. 26, no. 2, pp. 91–95, 2016.

[19] X. Ma, S. Chen, and F. Chen, "Multivariate space-time modeling of crash frequencies by injury severity levels," *Anal. Methods Accident Res.*, vol. 15, pp. 29–40, Sep. 2017.

[20] W. Chang, S. Qinyu, F. Rui, L. Zhen, and Z. Qiong, "Lane change warning threshold based on driver perception characteristics," *Accident Anal. Prevention*, vol. 117, pp. 164–174, Aug. 2018.

[21] A. Kondyli, A. Barmpoutis, V. P. Sisiopiku, L. Zhang, L. Zhao, M. M. Islam, S. S. Patil, and S. R. Hosuri, "A 3D body posture analysis framework during merging and lane-changing maneuvers," *J. Transp. Saf. Secur.*, vol. 10, no. 5, pp. 411–428, Apr. 2017.

[22] H. Yu, H. E. Tseng, and R. Langari, "A human-like game theory-based controller for automatic lane changing," *Transp. Res. C, Emerg. Technol.*, vol. 88, pp. 140–158, Mar. 2018.

[23] H. Park, C. Oh, J. Moon, and S. Kim, "Development of a lane change risk index using vehicle trajectory data," *Accident Anal. Prevention*, vol. 110, pp. 1–8, Jan. 2018.

[24] F. Chen and S. Chen, "Injury severities of truck drivers in single-and multi-vehicle accidents on rural highways," *Accident Anal. Prevention*, vol. 43, no. 5, pp. 1677–1688, Sep. 2011.

[25] L. Yang, X. Li, W. Guan, H. M. Zhang, and L. Fan, "Effect of traffic density on drivers' lane change and overtaking maneuvers in freeway situation—A driving simulator–based study," *Traffic Injury Prevention*, vol. 19, no. 6, pp. 594–600, 2018.

[26] J. Przybyla, J. Taylor, J. Jupe, and X. Zhou, "Estimating risk effects of driving distraction: A dynamic errorable car-following model," *Transp. Res. C, Emerg. Technol.*, vol. 50, pp. 117–129, Jan. 2015.

[27] J. Nie, J. Zhang, W. Ding, X. Wan, X. Chen, and B. Ran, "Decentralized cooperative lane-changing decision-making for connected autonomous vehicles*," *IEEE Access*, vol. 4, pp. 9413–9420, 2016.

[28] Z. C. He, Y. M. Wang, W. B. Sun, P. Y. Huang, L. C. Zhang, and R. X. Zhong, "Modelling car-following behaviour with lateral separation and overtaking expectation," *Transportmetrica B, Transp. Dyn.*, vol. 4, no. 3, pp. 223–239, Sep. 2015.

[29] L. Li, C. Lv, D. Cao, and J. Zhang, "Retrieving common discretionary lane changing characteristics from trajectories," *IEEE Trans. Veh. Technol.*, vol. 67, no. 3, pp. 2014–2024, Mar. 2018.

[30] C. Ma, R. He, and W. Zhang, "Path optimization of taxi carpooling," *PLoS ONE*, vol. 13, no. 8, Aug. 2018, Art. no. e0203221.

[31] K. Li, X. Wang, Y. Xu, and J. Wang, "Lane changing intention recognition based on speech recognition models," *Transp. Res. C, Emerg. Technol.*, vol. 69, pp. 497–514, Aug. 2016.

[32] L. Yun, Z. Hou, and D. Yu, "Driving intentions identification based on continuous P-2D HMM," in *Proc. 2nd Int. Conf. Digit. Manuf. Automat.*, Zhangjiajie, China, Aug. 2011, pp. 460–464.

[33] M. Jingjing and W. Yihu, "Driving intentions identification based on continuous pseudo 2D hidden Markov model," in *Proc. 5th Int. Conf. Intell. Comput. Technol. Automat.*, Zhangjiajie, China, Jan. 2012, pp. 629–632.

[34] Y. Zheng and J. H. L. Hansen, "Lane-change detection from steering signal using spectral segmentation and learning-based classification," *IEEE Trans. Intell. Vehicles*, vol. 2, no. 1, pp. 14–24, Mar. 2017.

[35] O. C. Puan, M. N. Ibrahim, and R. Zakaria, "Multiple logistic regression model of signalling practices of drivers on urban highways," in *Proc. AIP Conf.*, May 2015, pp. 135–136.

[36] C. Lee, P. Yong-Jin, and M. Abdel-Ary, "Effects of lane-change and car-following-related traffic flow parameters on crash occurrence by lane," presented at the Transp. Res. Board 88th Annu. Meeting, Washington, DC, USA, Jan. 2009.

[37] R. S. Tomar and S. Verma, "Trajectory predictions of lane changing vehicles using SVM," *Int. J. Vehicle Saf.*, vol. 5, no. 4, p. 345, Jan. 2011.

[38] E. Balal, R. L. Cheu, T. Gyan-Sarkodie, and J. Miramontes, "Analysis of discretionary lane changing parameters on freeways," *Int. J. Transp. Sci. Tech.*, vol. 2014, vol. 3, no. 3, pp. 277–296, Sep. 2014.

[39] C. Ma, W. Hao, A. Wang, and H. Zhao, "Developing a coordinated signal control system for urban ring road under the vehicle-infrastructure connected environment," *IEEE Access*, vol. 6, pp. 52471–52478, 2018.

[40] D. Kasper, G. Weidl, T. Dang, G. Breuel, A. Tamke, and W. Rosenstiel, "Object-oriented Bayesian networks for detection of lane change maneuvers," in *Proc. IEEE Intell. Vehicles Symp.*, Baden-Baden, Germany, Jun. 2011, pp. 673–678.

[41] J. Q. Wang, R. Chai, and N. Cao, "Modeling highway lane changing using Bayesian networks," *Appl. Mech. Mater.*, vols. 505–506, pp. 1143–1147, Jan. 2014.

[42] G. Xie, H. Gao, L. Qian, B. Huang, K. Li, and J. Wang, "Vehicle trajectory prediction by integrating physics-and maneuver-based approaches using interactive multiple models," *IEEE Trans. Ind. Electron.*, vol. 65, no. 7, pp. 5999–6008, Jul. 2018.

[43] P. Kumar, M. Perrollaz, S. Lefèvre, and C. Laugier, "Learning-based approach for online lane change intention prediction," in *Proc. IEEE Intell. Vehicles Symp.*, Gold Coast, QLD, Australia, Jun. 2013, pp. 797–802.

[44] Y. Hou, P. Edara, and C. Sun, "Situation assessment and decision making for lane change assistance using ensemble learning methods," *Expert Syst. Appl.*, vol. 42, no. 8, pp. 3875–3882, May 2015.

[45] J. Gao, Y. L. Murphey, and H. Zhu, "Multivariate time series prediction of lane changing behavior using deep neural network," *Appl. Intell.*, vol. 48, no. 10, pp. 3523–3537, Oct. 2018.

[46] G. Xu, L. Liu, Y. Ou, and Z. Song, "Dynamic modeling of Driver control strategy of lane-change behavior and trajectory planning for collision prediction," *IEEE Trans. Intell. Transp. Syst.*, vol. 13, no. 3, pp. 1138–1155, Sep. 2012.
[47] B. Morris, A. Doshi, and M. Trivedi, "Lane change intent prediction for driver assistance: On-road design and evaluation," in *Proc. IEEE Intell. Vehicles Symp.*, Baden-Baden, Germany, Jun. 2011, pp. 895–901.

TING XU was born in Xi'an, Shaanxi, China, in 1983. She received the B.S. degree in computer science and technology, the M.Sc. degree in traffic information engineering and control from Chang'an University, Xi'an, in 2005 and 2007, respectively, and the Ph.D. degree in transportation planning and management from the Beijing University of Technology, in 2011.

From 2011 to 2015, she was an Assistant Professor with the School of Automotive, Chang'an University, where she has been an Associate Professor, since 2015. She has published more than 30 articles, and 10 inventions patents. Her current research interests include roadway safety, data mining techniques, driving behavior, and so on.

CHANGLEI WEN was born in Ganzhou, Jiangxi, China, in 1996. He received the B.S. degree in vehicle operation engineering from Chang'an University, Xi'an, China, in 2018, where he is currently pursuing the master's degree in transportation planning and management. He has been the author of more than five articles. His current research interests include traffic safety and data mining.

LEI ZHAO was born in Weinan, Shaanxi, China, in 1994. He received the B.S. degree in vehicle operation engineering from Chang'an University, Xi'an, China, in 2016, where he is currently pursuing the Ph.D. degree in transportation planning and management. He has published more than five articles. His current research interests include traffic safety, public transportation, and autonomous vehicles.

MEIJUN LIU was born in Datong, Shan'xi, China, in 1992. She received the B.S. degree in vehicle operation engineering from Chang'an University, Xi'an, China, in 2014, where she is currently pursuing the master's degree in transportation engineering. Her research fields include traffic safety and driving behavior.

XIANG ZHANG was born in Bole Xinjiang, China, in 1994. She received the B.S. degree in vehicle operation engineering from Chang'an University, Xi'an, China, in 2018, where she is currently pursuing the master's degree in transportation planning and management. Her current research interests focuses on roadway safety, data mining, and machine learning techniques.